

Circ-SMO-encoded 193 a.a. Confers Chemotherapy Resistance and Immune Escape to Glioma Stem Cells

sheng yan

Sun Yat-sen University First Affiliated Hospital

shengyong wang

Guangxi Medical University First Affiliated Hospital

xixi li

Sun Yat-sen University First Affiliated Hospital

yibing yang

Sun Yat-sen University First Affiliated Hospital

xujia wu

Sun Yat-sen University First Affiliated Hospital

jian zhong

Sun Yat-sen University First Affiliated Hospital

junju chen

Sun Yat-sen University First Affiliated Hospital

zhipeng chen

Sun Yat-sen University First Affiliated Hospital

lin xu

Sun Yat-sen University First Affiliated Hospital

quan zhou

Sun Yat-sen University First Affiliated Hospital

xinya gao (✉ gaoxy36@mail.sysu.edu.cn)

Sun Yat-sen University First Affiliated Hospital <https://orcid.org/0000-0003-0629-7661>

Research Article

Keywords: CircRNA, Glioma, Circ-SMO-193aa, chemo-resistance, immune escape

Posted Date: June 10th, 2021

DOI: <https://doi.org/10.21203/rs.3.rs-583477/v1>

License:  This work is licensed under a Creative Commons Attribution 4.0 International License.

[Read Full License](#)

Abstract

Background: Emerging evidence indicates that circRNAs and their encoded proteins contribute to the tumorigenesis of glioma; however, the biological function and underlying mechanism of chemotherapy resistance and immune escape are largely known.

Methods: We applied qRT-PCR, western blotting and immunohistochemistry to detect the expression level and correlation between Bax and PDL1. We next applied an apoptosis assay to detect chemotherapy resistance and immune escape.

Results: Circ-SMO and 193 a.a. were upregulated in temozolomide-resistant tumours and tumour-associated immune escape tumours. Circ-SMO and 193 a.a. inhibited temozolomide-induced cell death and promoted PDL1 expression.

Conclusion: Circ-SMO and 193 a.a. promote chemotherapy resistance and immune escape by modulating autophagy and PDL1 expression.

Introduction

Glioma is the most lethal malignancy in the central nervous system[1]. To date, temozolomide is the only adjuvant therapy medicine. However, although temozolomide improves patients' overall survival, rapid resistance has been reported in cells and patients treated with temozolomide[1, 2]. The mechanism is largely unknown, thus restricting the application of temozolomide. This issue urgently needs to be solved.

Autophagy is a critical programme in which cells collect misfolded proteins and injured organelles and send them to lysosomes for recycling[3]. However, this programme is tightly controlled in cells. Uncontrolled or uncontrolled autophagy was reported to be engaged in the tumorigenesis and progression of tumours[4, 5]. Autophagy is a double-edged sword; it recycles proteins and materials for further cellular programmes, but excessive autophagy leads to apoptosis, which is called "lethal autophagy".

circRNAs represent the majority of noncoding RNAs. circRNAs are closed, single-stranded, circular transcripts that lack 5' caps and 3' poly(A) tails[6]. Thus, circRNAs are considered not to translate conventionally. However, with advances in high-throughput sequencing, circRNAs have been shown to harbour mature m6A binding sites and ribosome entrance sequences (IRESs)[7, 8]. circRNAs were reported to translate into proteins and exert biological functions. In glioma, circ-FBXW7 and circ-SHPRH[9, 10] encode proteins that affect tumorigenesis post-translationally. Recent evidence has indicated that Circ-E-Cadherin encodes a novel ligand that activates EGFR/EGFRviii and thus promotes the self-renewal of glioblastoma[11]. Our recent research showed that circRNA Circ-SMO and its encoded protein promote the self-renewal of glioma stem cells by activating hedgehog-HH pathways[12]. However, chemotherapy resistance and tumour-associated immune escape were key factors affecting survival. This needs to be further illustrated.

In this study, we analysed the expression levels of Circ-SMO and 193 a.a. and the correlations between temozolomide (TMZ) -induced apoptosis and PDL1 expression. The results showed that Circ-SMO and 193 a.a. inhibited TMZ-induced apoptosis and activated PDL1 expression, thus inhibiting cytotoxic T cells.

Materials And Methods

Patients and species

Tissue samples and adjacent normal tissues were obtained from patients who underwent surgery at the First Affiliated Hospital of Guangxi Medical University between January 2013 and December 2014. All tissue samples were confirmed by pathology. This study was approved by the Ethics Committee of the First Affiliated Hospital of Guangxi Medical University and conformed to the 1964 Declaration of Helsinki and its later amendments or comparable ethical standards. Clinical samples were collected from patients after written informed consent was obtained.

Cells and cell culture

The GSC456, GSC4121, GSC387, and GSC3691 were gifts from UCSD. GSCs were cultured in DMEM/F12 medium with B27 and bFGF and EGF (20 ng ml⁻¹ each).

IHC

All tissues were paraffin embedded and cut into 8-10 µm slices. After deparaffinization and antigen restoration, the primary antibody was diluted in BSA and applied overnight at 4°C. After incubation with the secondary antibodies, diaminobenzidine was added to these tumour sections, which were then counterstained with haematoxylin to visualize nuclei. The score of the IHC staining was measured according to the percentage of positive cells and staining intensity. A score of 0-6 was considered low expression, while a score of 7-12 was considered high expression.

WB

Tumours and cells were lysed by RIPA with protease inhibitor. After quantification, equal amounts of proteins were subjected to SDS-PAGE, and after electrophoresis, the proteins were transferred to a transmembrane and blocked. Primary antibody was added overnight at 4°C. After washing, secondary antibody was applied, and the signals were visualized by chemiluminescence.

qRT-PCR

Tissues and cells were lysed with TRIzol reagent following the manufacturer's instructions. After reverse-transcription, the DNA was then amplified with specific primers. For Circ-SMO, the sequence was described as previously.

Apoptosis assay

Cells with the indicated modifications were subjected to apoptosis assays following the manufacturer's instructions. Cells were stained, and the apoptosis rate was detected.

Plasmid construction and stable cell establishment

Junction-specific shRNAs and overexpression plasmids were described previously. After harvesting the lentivirus, cells were transduced with lentivirus using polybrene (8 mg ml^{-1}). After incubation for 3 days, a stable cell line was successfully established.

IF

Cells were fixed and blocked and then incubated with primary antibodies overnight. After washing 3 times, a secondary antibody was applied, and DAPI was used for nuclear counterstaining. Images were taken using an Olympus FV1000 microscope.

Cell viability

Certain numbers of cells were seeded into the plate and incubated with cytotoxic T cells. CCK-8 was added to the plate, and the absorption was measured at 450 nm.

LDH detecting assay

The LDH level in the medium was measured using ELISA kits following the manufacturer's instructions. The LDH level was then normalized to the control.

Xenograft assay

Mice were randomly assigned to experimental groups for all experiments. For the animal survival analysis, mice were intracranially injected with 2,000 GSCs in $5 \mu\text{l}$ PBS and maintained until pathological symptoms from tumour burden developed or 70 days after injection. Tumour volume was then calculated.

Results

Circ-SMO and 193 a.a. are positively correlated with temozolomide (TMZ) resistance

We previously found that Circ-SMO and its encoded protein 193 a.a. promote the self-renewal of GSCs. To further uncover the biological function on TMZ resistance in glioma, we analysed the expression of Circ-SMO and apoptosis markers, such as Bax and cleaved caspase-3. The antibody for 193 a.a. was not suitable for immunohistochemistry assays; therefore, we applied qRT-PCR to measure the expression of Circ-SMO and used the mean value of the whole cohort as the cut-off. The results are shown in Figure 1A. In Circ-SMO low patients, Bax and cleaved caspase 3 were higher than in Circ-SMO high patients.

Regression analysis between Circ-SMO and BAX and cleaved caspase IHC scores indicated that Circ-SMO was negatively correlated with Bax and cleaved caspase 3. We next analysed the protein levels of 193 a.a., Bax and cleaved caspase 3. We next collected 4 samples before/after receiving TMZ treatment. We applied qRT-PCR and immunoblotting to detect Circ-SMO and 193 a.a., and the results showed that Circ-SMO and 193 a.a. increased with the application of TMZ in 3 samples. We next treated GSCs with TMZ and established TMZ-resistant cells. Circ-SMO and 193 a.a. increased in TMZ-resistant cells.

193 a.a. inhibits TMZ-induced apoptosis

We first established stable knockdown cell lines in 456 and 3691 cell lines and an overexpression cell line in 387 cells. We next treated the cells with TMZ and detected the apoptosis rate. The results showed that the apoptosis rate increased with Circ-SMO knockdown but decreased in Circ-SMO-overexpressing cells. We next detected the DNA damage marker g-H2A. X and the apoptosis markers Bax, cleaved caspase 3 and cleaved PARP. The results showed that g-H2A. X, cleaved caspase 3 and cleaved PARP increased in 456 and 3691 knockdown cell lines.

193 a.a. induces autophagy during TMZ resistance

Autophagy is one of the key mechanisms of TMZ resistance. We next detected LC3B-I/II and found that the ratio of LC3B-II/LC3B-I decreased in the Circ-SMO knockdown cell line. IF assays indicated that LC3B puncta decreased in Circ-SMO knockdown cell lines. However, a decrease in LC3B can result from a decrease in production or an increase in consumption. We next detected P62 expression, which is a key basic reagent for the fusion of autophagic vesicles and lysosomes. The results showed that P62 accumulated in the Circ-SMO knockdown cell line, indicating that autophagic flux decreased.

193 a.a.-induced autophagy is critical for cell survival

We previously indicated that 193 a.a. maintains autophagic flux to exert TMZ resistance. We next applied the autophagy activator rapamycin and autophagy inhibitor bafilomycin A1 (Baf1) for rescue experiments. The results showed that autophagic flux was completely restored after the application of rapamycin and bafilomycin A1. We next treated cells with TMZ and subjected the cells to apoptosis detection assays. The results showed that the apoptosis rate and apoptosis markers were completely restored in the rescue cell line, indicating that 193 a.a. exert its function in an autophagy-dependent manner.

Targeting Circ-SMO sensitizes GSCs to TMZ in vivo

We next investigated the biofunction of Circ-SMO on TMZ resistance in vivo. We established xenograft models by injecting GSCs in situ and treating them with TMZ. Tumours were collected following the protocol, and the tumour volume and overall survival analysis were measured. The results showed that knocking down Circ-SMO inhibited tumorigenesis and thus prolonged the overall survival period.

Circ-SMO-induced PDL1 expression confers tumour-associated immune escape to GSCs

Tumour-associated immune therapy is a hot fields. Targeting PD1/PDL1 has a great effect in immunotherapy. We next detected the expression correlation between Circ-SMO and PDL1. The results showed that Circ-SMO was positively correlated with PDL1, and samples with higher levels of Circ-SMO harboured high levels of PDL1. PDL1 plays a primary role in inhibiting cytotoxic CD8⁺ T cell infiltration. We next detected the cytotoxic CD8⁺ T cell marker CD8. The infiltration fraction of CD8⁺ T cells decreased in higher Circ-SMO patients. We next detected PDL1 levels in a stable cell line. PDL1 decreased with the knockdown of Circ-SMO. We next coincubated GSCs with cytotoxic T cells and detected the relative cell viability and LDH level in suspension. The results showed that cell viability decreased, while the apoptosis marker LDH increased in Circ-SMO knockdown cells.

Circ-SMO-induced Gli1/3 activation is responsible for PDL1 expression

To further uncover the underlying mechanism of Circ-SMO on the expression of PDL1, we first detected the Gli1/3 level and established a rescue cell line. We re-expressed Gli1/3 in stable knockdown cell lines, and we knocked down Gli1/3 in Circ-SMO-overexpressing cells. Gli1/3 and PDL1 were detected for confirmation. We next cocultured the cells with cytotoxic cells and subjected them to CCK-8 and LDH detection assays. The results showed that PDL1 was completely restored with the rescue of Gli1/3 and that Circ-SMO-induced immune inhibition was also restored.

Discussion

Glioma is the most lethal malignancy in the central nervous system[13]. To date, temozolomide is still the only adjuvant medicine. Spatial analysis indicated that the in the tumour is responsible for TMZ resistance[14]. Glioma stem cells play key roles in resistance to chemotherapy and radiotherapy[15]. Gliomas develop rapid resistance through multiple pathways. Epigenetic regulation plays a critical role in acquiring resistance to TMZ. PARP-mediated PARYlation of MGMT promotes the repair of temozolomide-induced O6-methylguanine DNA damage and thus promotes cell survival[16]. EIF4A3-induced circular RNA ASAP1 promotes tumorigenesis and temozolomide resistance of glioblastoma via NRAS/MEK1/ERK1-2 signalling[17]. TGF- β 1 modulates temozolomide resistance in glioblastoma via altered microRNA processing and elevated MGMT[18]. Increased activation of HDAC1/2/6 and Sp1 underlies therapeutic resistance and tumour growth in glioblastoma[19]. DNA methylation-mediated activation of lncRNA SNHG12 promotes temozolomide resistance in glioblastoma. Autophagy contributes to the resistance of TMZ[20]. Studies have shown that disruption of the inherent autophagic flux senses cells to TMZ. Berberine reduces temozolomide resistance by inducing autophagy via the ERK1/2 signalling pathway in glioblastoma[21]. Knockdown of lncRNA DLEU1 inhibits glioma progression and promotes temozolomide chemosensitivity by regulating autophagy[22]. TOPK inhibits autophagy by phosphorylating ULK1 and promotes glioma resistance to TMZ[23]. However, the underlying mechanism remains unknown, and no targets are available to overcome TMZ resistance.

Anti-PDL1/PD1-based immune therapy comprises the majority of immunotherapies. However, the clinical trial glioma results were disappointing. The reasons may be attributed to the unique microenvironment of

the brain[24]. However, understanding the regulation of PDL1/PD1 and the mechanism of tumour-associated immune escape is urgently needed.

In this study, we found that Circ-SMO and 193 a.a. confer TMZ resistance to GSCs by modulating autophagy. Interrupting the autophagy change resensitized GSCs to TMZ. Circ-SMO and 193 a.a. were previously reported to activate HH pathways. We further indicated that 193 a.a. induces PDL1 overexpression in a Gli1/3-dependent manner.

Conclusion

Our research indicated that Circ-SMO and 193 a.a. promote chemotherapy resistance and immune escape by modulating autophagy and PDL1 expression. This research further uncover the potential mechanism of Circ-SMO-193aa on the progression of glioblastoma and the mechanism of TMZ resistance and tumor associated immune escape in glioblastoma.

Abbreviations

qRT-PCR:quantative real time poly chain reaction

IRES: ribosome entrance sequence

HH: hedgehog

TMZ: temozolomide

GSC: glioma stem cell

Baf1: bafilomycin A1

Declarations

Ethics approval and consent to participate

Studies were performed conforming to the Declaration of Helsinki and got approval the Ethics Committee of the First Affiliated Hospital of Guangxi Medical University. Clinical samples were collected from patients after written informed consent was obtained. The animal studies were approved by the Laboratory Animal Care committee of The First Affiliated Hospital of Sun Yat-sen University.

Consent for publication

Not applicable

Acknowledgements

We thanked a lot for the patients involved in this article.

Competing interests

The authors declare no competing interests.

Availability

All data was available in this article.

Funding

This work was supported in part by the National Natural Science Foundation of China [81902524], the Basic and applied Foundation of Guangdong (2020A1515110689).

Author contribution

QZ and XYG designed the article. All the authors were engaged in the experiments application, data collection and analysis, literal writing and editing.

References

1. Reifenberger, G., et al., *Advances in the molecular genetics of gliomas - implications for classification and therapy*. Nat Rev Clin Oncol, 2017. **14**(7): p. 434-452.
2. Lo Dico, A., et al., *Role of Metformin and AKT Axis Modulation in the Reversion of Hypoxia Induced TMZ-Resistance in Glioma Cells*. Front Oncol, 2019. **9**: p. 463.
3. Deane, C., *Compromised autophagy*. Nat Chem Biol, 2021. **17**(6): p. 626.
4. Talukdar, S., et al., *Autophagy and senescence: Insights from normal and cancer stem cells*. Adv Cancer Res, 2021. **150**: p. 147-208.
5. Patel, N.H., et al., *Autophagy and senescence in cancer therapy*. Adv Cancer Res, 2021. **150**: p. 1-74.
6. Bozzoni, I., *Widespread occurrence of circular RNA in eukaryotes*. Nat Rev Genet, 2021.
7. Zhang, L., et al., *The role of N(6)-methyladenosine (m(6)A) modification in the regulation of circRNAs*. Mol Cancer, 2020. **19**(1): p. 105.
8. Lei, M., et al., *Translation and functional roles of circular RNAs in human cancer*. Mol Cancer, 2020. **19**(1): p. 30.
9. Yang, Y., et al., *Novel Role of FBXW7 Circular RNA in Repressing Glioma Tumorigenesis*. J Natl Cancer Inst, 2018. **110**(3).
10. Begum, S., et al., *Novel tumour suppressive protein encoded by circular RNA, circ-SHPRH, in glioblastomas*. Oncogene, 2018. **37**(30): p. 4055-4057.
11. Gao, X., et al., *Circular RNA-encoded oncogenic E-cadherin variant promotes glioblastoma tumorigenicity through activation of EGFR-STAT3 signalling*. Nat Cell Biol, 2021. **23**(3): p. 278-291.

12. Wu, X., et al., *A novel protein encoded by circular SMO RNA is essential for Hedgehog signaling activation and glioblastoma tumorigenicity*. Genome Biol, 2021. **22**(1): p. 33.
13. Aldape, K., et al., *Challenges to curing primary brain tumours*. Nat Rev Clin Oncol, 2019. **16**(8): p. 509-520.
14. Jovanovic, M., et al., *Novel TrxR1 Inhibitors Show Potential for Glioma Treatment by Suppressing the Invasion and Sensitizing Glioma Cells to Chemotherapy*. Front Mol Biosci, 2020. **7**: p. 586146.
15. Wang, S.M., et al., *CCAAT/Enhancer-binding protein delta mediates glioma stem-like cell enrichment and ATP-binding cassette transporter ABCA1 activation for temozolomide resistance in glioblastoma*. Cell Death Discov, 2021. **7**(1): p. 8.
16. Wu, S., et al., *PARP mediated PARylation of MGMT is critical to promote repair of temozolomide-induced O6-methylguanine DNA damage in glioblastoma*. Neuro Oncol, 2021.
17. Wei, Y., et al., *EIF4A3-induced circular RNA ASAP1 promotes tumorigenesis and temozolomide resistance of glioblastoma via NRAS/MEK1/ERK1-2 signaling*. Neuro Oncol, 2021. **23**(4): p. 611-624.
18. Nie, E., et al., *TGF-beta1 modulates temozolomide resistance in glioblastoma via altered microRNA processing and elevated MGMT*. Neuro Oncol, 2021. **23**(3): p. 435-446.
19. Yang, W.B., et al., *Increased activation of HDAC1/2/6 and Sp1 underlies therapeutic resistance and tumor growth in glioblastoma*. Neuro Oncol, 2020. **22**(10): p. 1439-1451.
20. Lu, C., et al., *DNA-methylation-mediated activating of lncRNA SNHG12 promotes temozolomide resistance in glioblastoma*. Mol Cancer, 2020. **19**(1): p. 28.
21. Qu, H., et al., *Berberine reduces temozolomide resistance by inducing autophagy via the ERK1/2 signaling pathway in glioblastoma*. Cancer Cell Int, 2020. **20**(1): p. 592.
22. Lv, Q.L., et al., *Knockdown lncRNA DLEU1 Inhibits Gliomas Progression and Promotes Temozolomide Chemosensitivity by Regulating Autophagy*. Front Pharmacol, 2020. **11**: p. 560543.
23. Lu, H., et al., *TOPK inhibits autophagy by phosphorylating ULK1 and promotes glioma resistance to TMZ*. Cell Death Dis, 2019. **10**(8): p. 583.
24. Berghoff, A.S. and M. Preusser, *Does neoadjuvant anti-PD1 therapy improve glioblastoma outcome?* Nat Rev Neurol, 2019. **15**(6): p. 314-315.

Figures

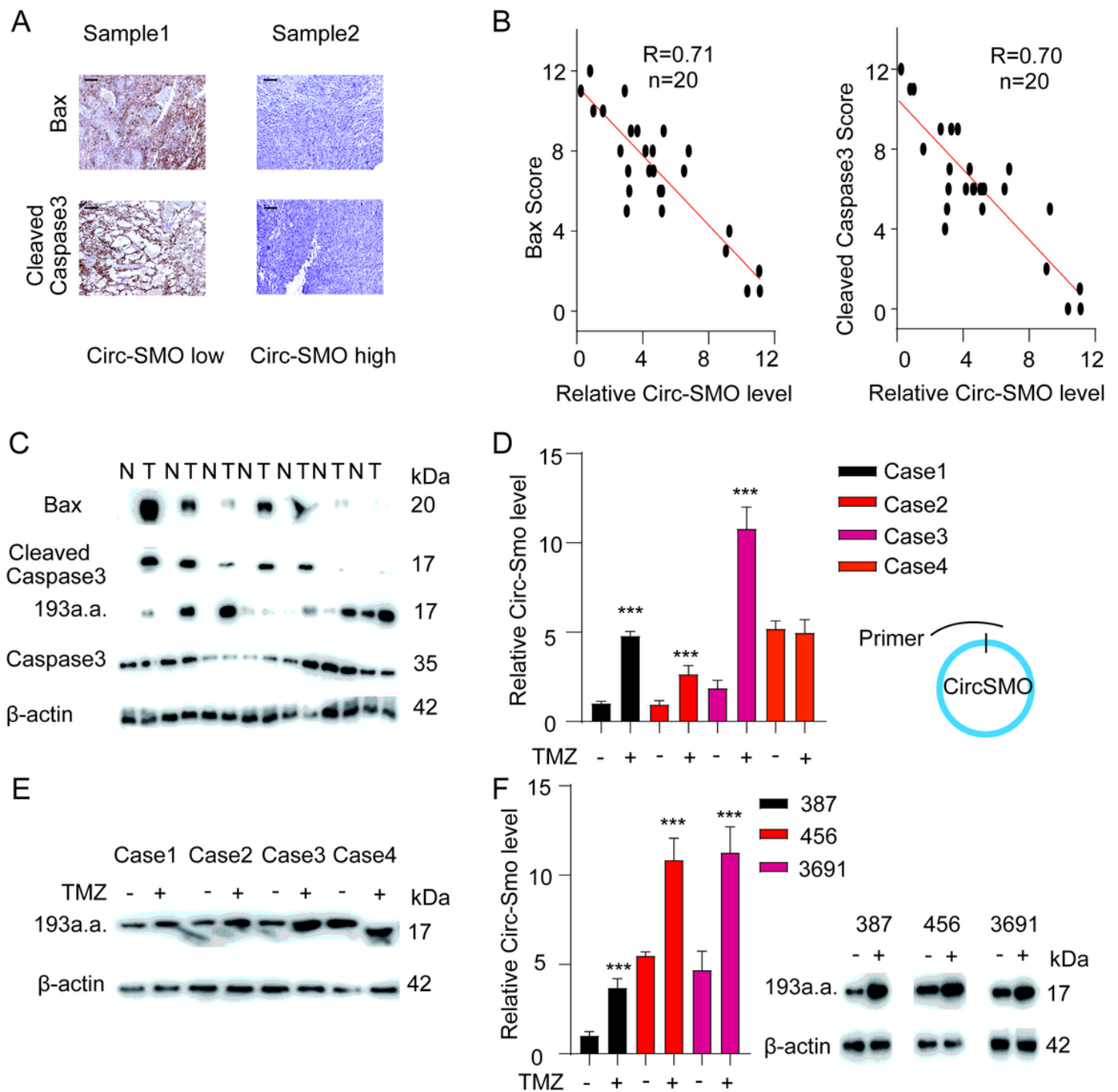


Figure 1

Circ-SMO and 193 a.a. are correlated with TMZ resistance A: Patients in our in-house cohort were divided into high and low groups, with the mean level of Circ-SMO as the cut-off. IHC was applied to measure the expression of Bax and cleaved caspase 3. Scale, 200 μ m. B: Regression analysis of the IHC scores of Bax and cleaved caspase 3 and the level of Circ-SMO in our in-house database. The data were obtained from A. C: Seven paired glioma and paired normal tissues were selected. Immunoblotting was applied to measure Bax, 193 a.a. and cleaved caspase 3. D: Four samples before/after TMZ treatment were enrolled, and the relative RNA and protein levels were detected (E),^{***}, $p<0.001$. F: GSCs 387, 456, and 3691 were treated with TMZ, and the levels of Circ-SMO and 193 a.a. were detected,^{***}, $p<0.001$.

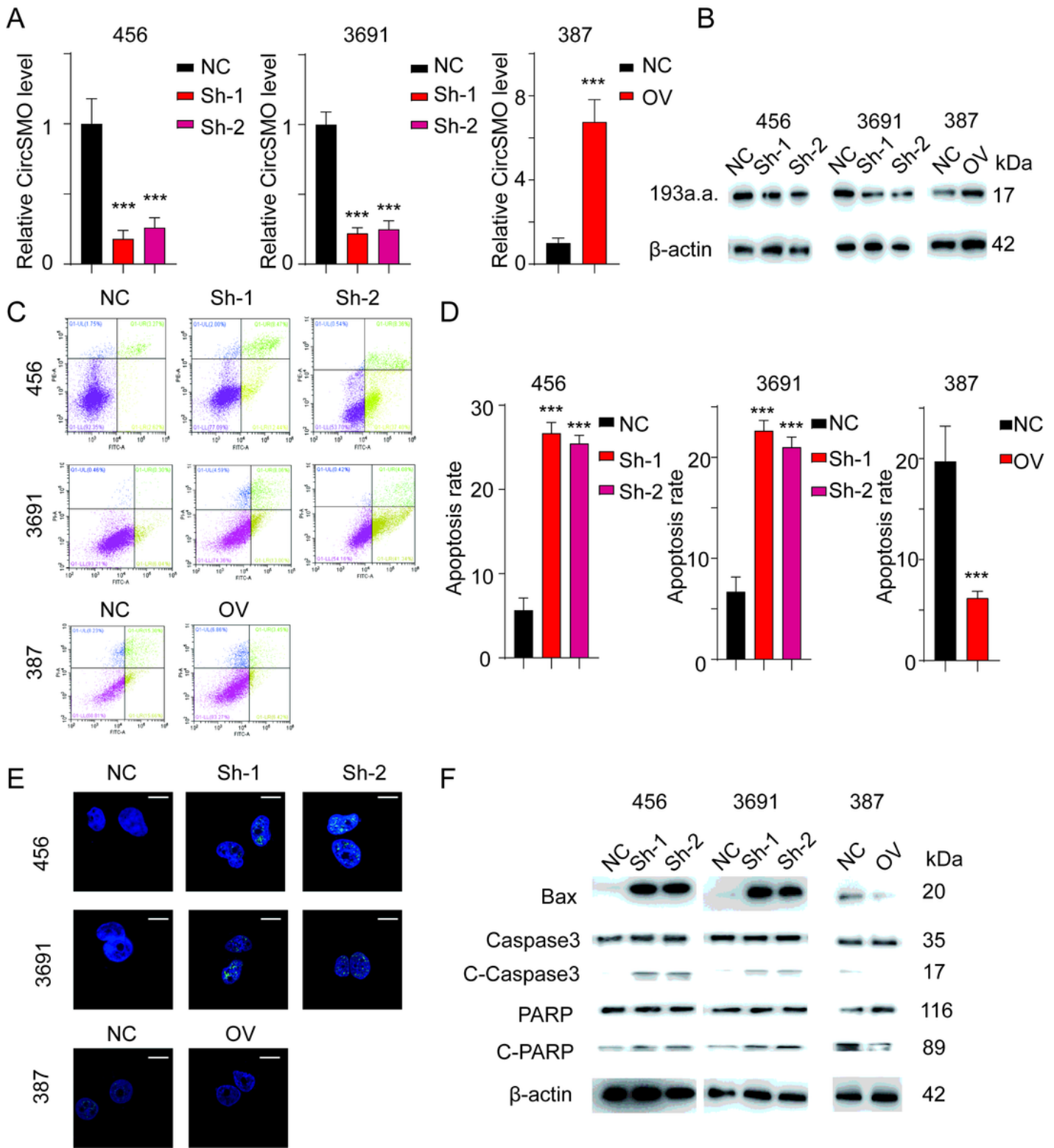


Figure 2

Circ-SMO and 193 a.a. inhibit TMZ-induced cell death in GSCs 456 and 3691 cells were transfected with shRNAs; after establishing stable cell lines, the relative RNA level (A) and protein level (B) were detected. After treatment with TMZ, the cells were then subjected to apoptosis assays. Flow cytometry (C) and the apoptosis rate (D) were detected,***, $p < 0.001$. E: Immunofluorescence of γ -H2A. X was detected in cells with the indicated modifications, scale 200 μ m. F: The apoptosis marker was measured.

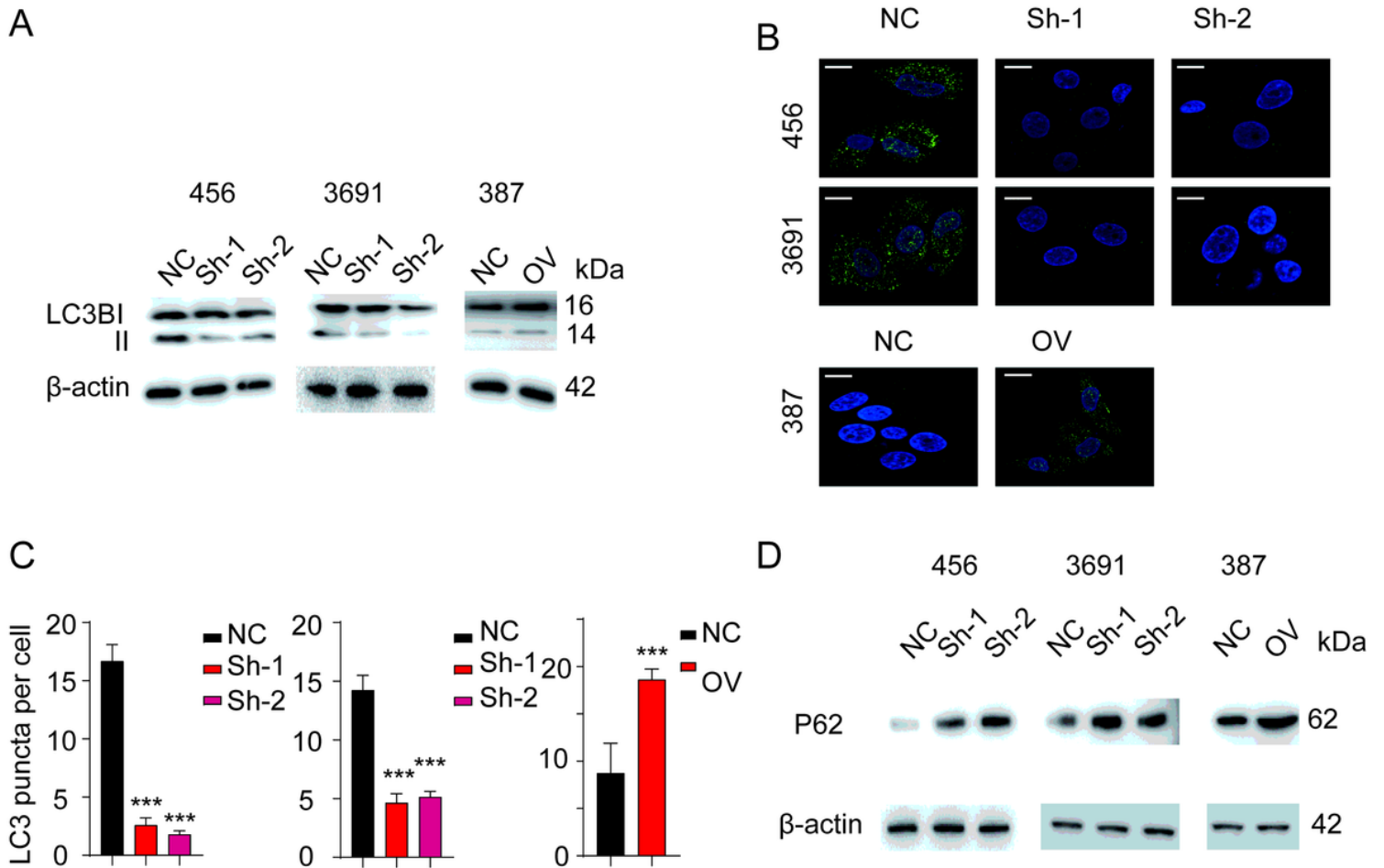


Figure 3

Circ-SMO and 193 a.a. induce autophagy in GSCs A: Immunoblotting of LC3B in different cell lines. B: Immunofluorescence of LC3B in cells with the indicated modification. The statistical analysis of LC3B puncta is shown in C, scale, 200 μ m,***,p<0.001. D: Immunoblotting of P62 in cells with the indicated modifications.

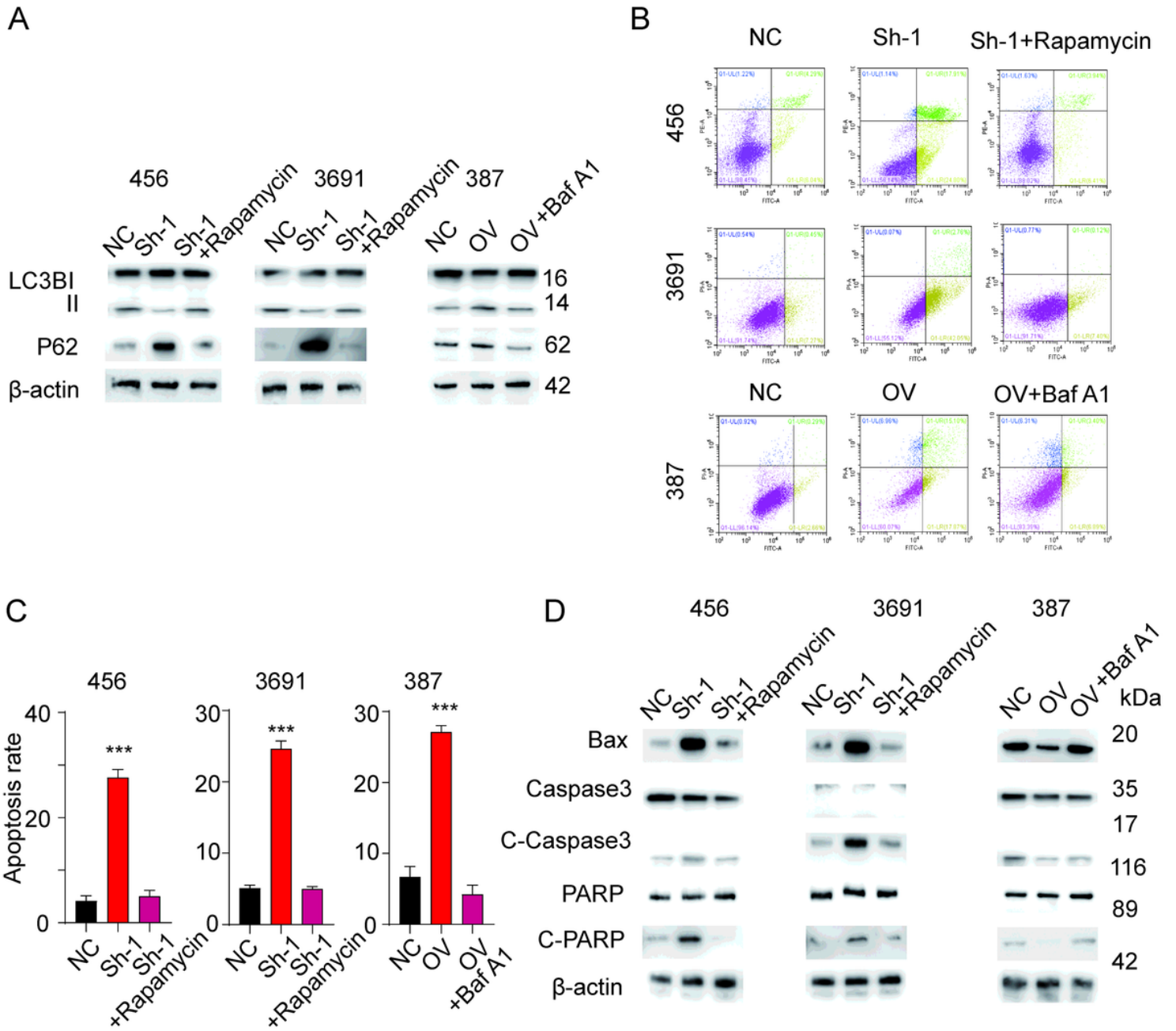


Figure 4

Circ-SMO and 193 a.a. promote cell survival in an autophagy-dependent manner. A: Rescue cell lines were established, and LC3B and P62 were detected. B: Rescue cell lines were subjected to apoptosis assays, and flow cytometry is shown. C: The apoptosis rate was detected,***, $p < 0.001$. D: The apoptosis marker was measured.

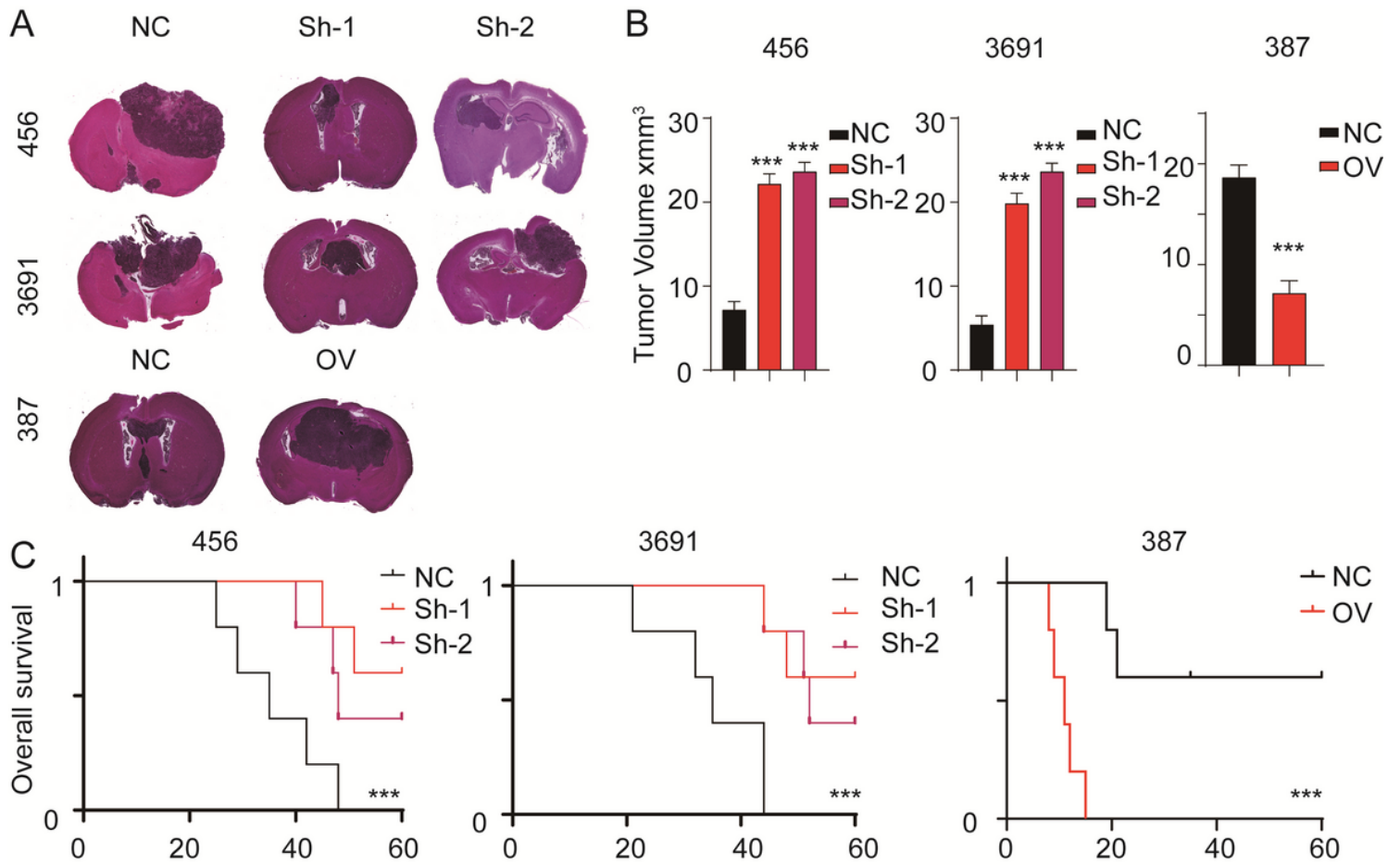


Figure 5

Circ-SMO and 193 a.a. confer TMZ resistance to GSCs in vivo A: Representative image of the xenograft assay. B: The tumour volume of different cell lines,***,p<0.001. C: The overall survival analysis was applied,***,p<0.001.

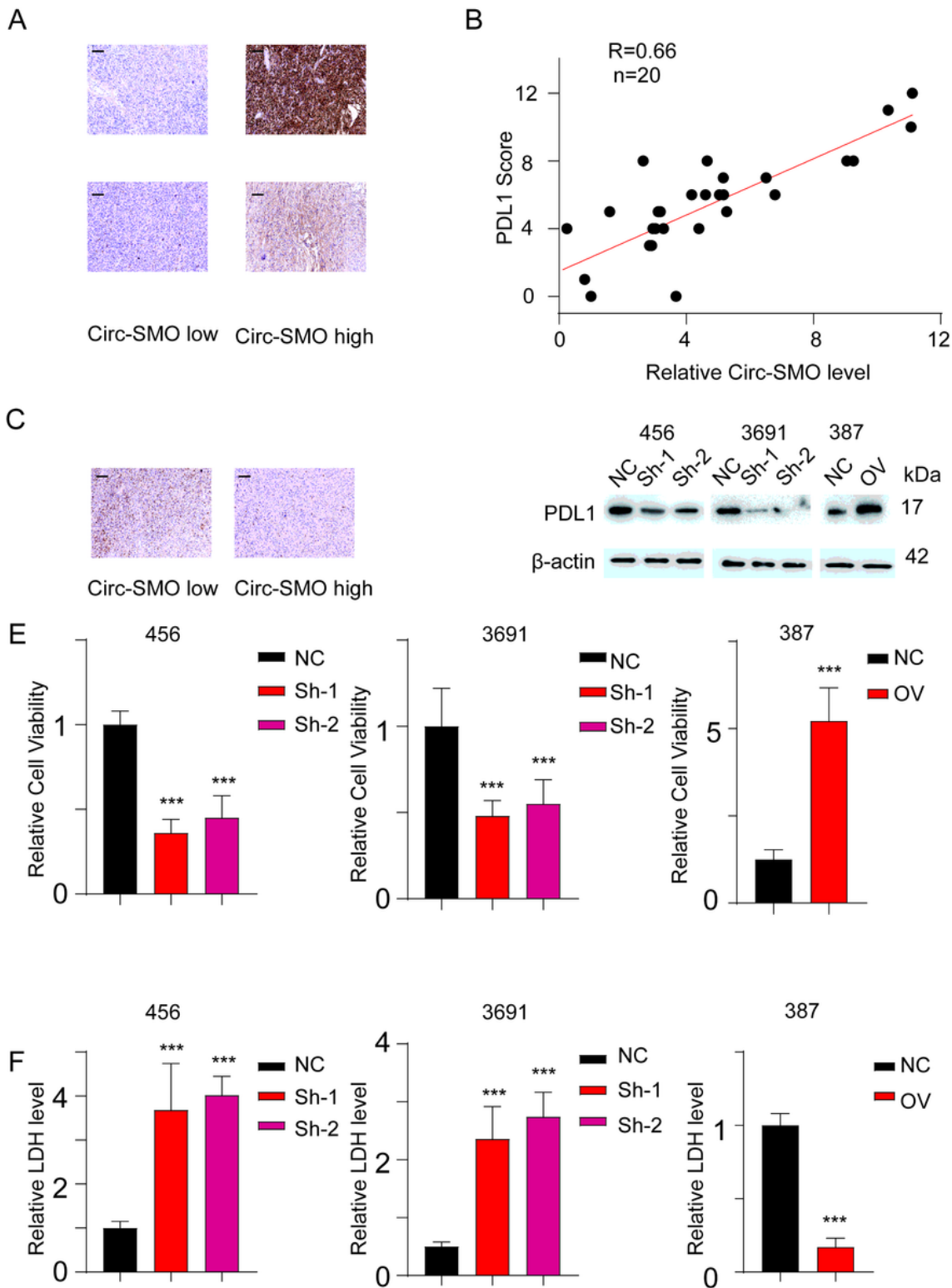


Figure 6

Circ-SMO and 193 a.a. induce PDL1 expression and tumour escape A: IHC of PDL1 in our in-house database, scale, 200 μ m,. B: Regression analysis of PDL1 and relative Circ-SMO level. C: IHC of CD8 in the glioma samples, scale, 200 μ m,. D: Immunoblotting of PDL1 in different cell lines. E: GSCs were incubated with cytotoxic CD8 T cells, and the relative cell viability (E) and LDH level in suspension (F) were detected,***, $p<0.001$.

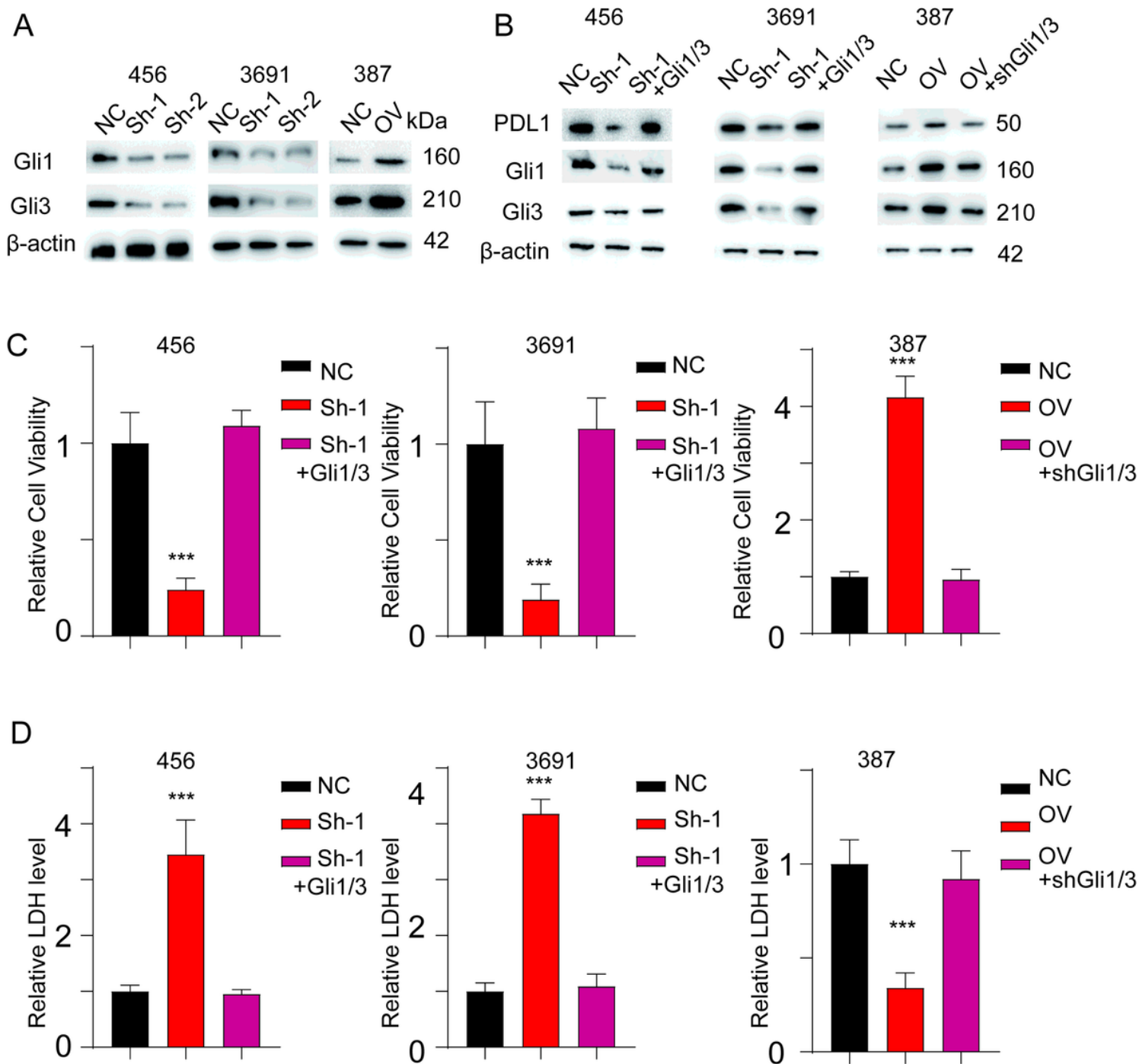


Figure 7

Circ-SMO and 193 a.a. maintain PDL1 expression in a Gli1/3-dependent manner. A: Immunoblotting of Gli1/3 was detected in cells with the indicated modifications. B: Rescue cell lines were established with Gli1/3 shRNA and overexpression at 456, 3691 and 387. C: Rescue GSCs were incubated with cytotoxic CD8 T cells, and the relative cell viability (c) and LDH level in suspension (D) were detected,***, $p < 0.001$.